American Mineralogist, Volume 83, pages 872–880, 1998

Characterization of the high-temperature modifications of incommensurate tridymite L3-T_O(MX-1) from 25 to 250 °C

HERIBERT GRAETSCH*

Institut für Mineralogie, Ruhr-Universität Bochum, D-44780 Bochum, Germany

ABSTRACT

Incommensurate tridymite L3-T_O(MX-1) shows a cascade of five phase transitions at 65, 110, 150, 200, and 380 °C upon heating. The X-ray diffraction patterns were investigated with a Buerger precession camera revealing a sequence of four incommensurate phases in the range from room temperature to 200 °C. The phases formed between 65 and 110 °C and between 110 and 150 °C are new modifications of tridymite. At 65 °C the monoclinic tridymite L3-T_O(MX-1) phase undergoes a first-order transformation to an orthorhombic phase. The incommensurate structural modulation of the room-temperature phase with the wavevector $\mathbf{q}_1 = 0.663\ \mathbf{a}^* - 0.498\ \mathbf{c}^*$ flips to $\mathbf{q}_2 = 0.042\ \mathbf{a}^* - 0.388\ \mathbf{c}^*$. Simultaneously, a commensurate modulation with tripled *b* lattice parameter is formed. The wavelengths of both modulations do not depend appreciably on the temperature. The incommensurate modulation discontinuously disappears near 110 °C whereas the commensurate modulation along the **b** axis becomes non-integral with a temperature-dependent wavelength varying between 115 and 100 Å. At 150 °C the symmetry is reduced to monoclinic again with $\gamma = 90.4°$. Between 150 and 200 °C the monoclinic angle gradually decreases to 90° and the wavelength of the modulation from about 90 to 65 Å. At higher temperatures, the satellite reflections fade into weak streaks and the normal orthorhombic high-temperature modification of tridymite is formed.

The phase transitions are reversible upon cooling except for the first transformation that is partly irreversible for single crystals and reversible but incomplete for pulverized material at room temperature.

INTRODUCTION

There are at least three modifications of tridymite known to exist at room temperature with different superstructures: ordered monoclinic tridymite L1-T_O(MC) with $a_{hex} \times 3\sqrt{3}\ a_{hex} \times 6\ c_{hex}$ in pseudo-orthohexagonal setting (Kato and Nukui 1976), stacking disordered pseudo-orthorhombic L2-T_D($PO_{5/10}$) with $2\ a_{hex} \times 2\sqrt{3}\ a_{hex} \times 10\ c_{hex}$ (Konnert and Appleman 1978) and incommensurate monoclinic tridymite L3-T_O(MX-1) with $a_{hex} \times \sqrt{3}\ a_{hex} \times c_{hex}$ for the average structure (Hoffmann et al. 1983), where a_{hex} and c_{hex} are the lattice parameters of the hexagonal high-temperature modification of tridymite. The nomenclature is a merger of those of Löns and Hoffmann (1987) and Flörke and Nukui (1988) and of Nukui et al. (1978) in parenthesis (for explanation see Table 1). All forms of tridymite consist of a framework of six-membered rings of corner-sharing SiO_4^{2-} tetrahedra (Fig. 1). The structural differences can most easily be described as distortions of the shape of the six-membered rings that have a hexagonal shape in hexagonal high-temperature tridymite but are oval in L2–T_D($PO_{5/10}$) (Konnert and Appleman 1978) and ditrigonal in L3–T_O(MX-1) (Löns and Hoffmann 1987). In L1-T_O(MC) both oval and ditrigonal rings occur (Kato and Nukui 1976; Dollase and Baur 1976; Baur 1977).

Several intermediate phases are formed upon cooling hexagonal tridymite before the respective room-temperature modifications are obtained. According to Nukui et al. (1978), the transformation sequence of synthetic monoclinic tridymite L1-T_O(MC) consists of five phases (see Table 1). It should be noted that there is no group-subgroup relationship between the room-temperature modification L1-T_O(MC) and the intermediate orthorhombic phase H4-T_O(OP) (Dollase and Baur 1976). L1-T_O(MC) crystals are usually twinned consisting of two or more individuals (Hoffmann 1967; Dollase and Baur 1976; Kato and Nukui 1976; Tagai et al. 1977).

However, some deviations from this transformation sequence have been reported more recently. De Dombal and Carpenter (1993) and Cellai et al. (1994) found evidence of an additional phase transition at 450 °C without change of the hexagonal crystal system. Dollase (1967) and Cellai et al. (1994) reported that on heating monoclinic tridymite from the Steinbach meteorite, it directly transforms to the H3-T_O(OS) phase at about 100 °C leaving out the intermediate H4-T_O(OP) phase. Using X-ray powder diffraction, Graetsch and Flörke (1991) found that the incommensurate H3-T_O(OS) phase slightly deviates from

* E-mail: heribert.graetsch@ruhr-uni-bochum.de

TABLE 1. Transformation sequence of tridymite L1-T_O (MC) upon heating according to Nukui et al. (1978)

Transition temperature (°C)	Phase	Space group of the basic structure	Wave vector of the modulation
	H1-T_O (HP)*	$P6_3/mmc$	—
380			
	H2-T_O (OC)†	$C222_1$	—
190			
	H3-T_O (OS)‡	$C112_1$	$\delta_b b^*$; δ_b = 0.09 to 0.13
150			
	H4-T_O (OP)§	$P2_12_12_1$	1/3 b*
110			
	L1-T_O (MC)‖	Cc	superstructure

Note: H = high temperature, L = low temperature, $_O$ = ordered; in parentheses: H = hexagonal, O = orthorhombic, M = monoclinic, P = primitive cell, C = C-centered, S = (incommensurate) superstructure.
* Gibbs (1927); Kihara (1978).
† Dollase (1967); Kihara et al. (1986a).
‡ Nukui et al. (1979); Graetsch and Flörke (1991).
§ Nukui et al. (1978); Kihara (1977).
‖ Kato and Nukui (1976); Dollase and Baur (1976); Baur (1977).

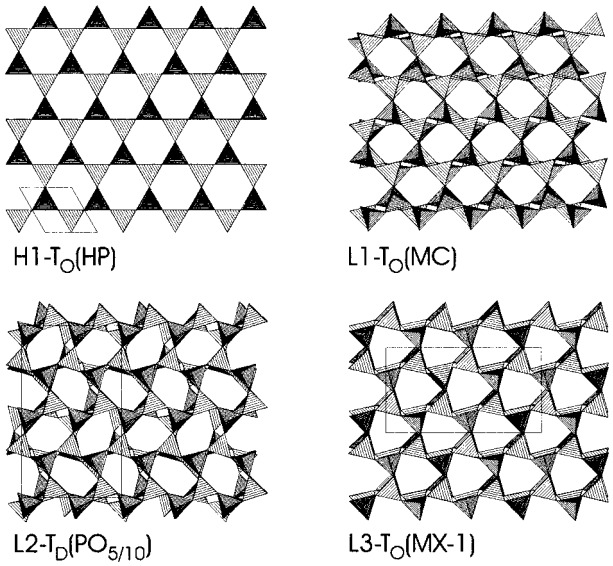

FIGURE 1. Polyhedral models of the three room-temperature modifications of tridymite and of hexagonal high-temperature tridymite in projection along the pseudohexagonal *c* axis.

orthorhombic symmetry by having a small monoclinic angle of 90.3°.

Furthermore, upon heating ordered monoclinic tridymite L1–T_O(MC) above the first transformation temperature and subsequent quenching to a temperature below 0 °C, a new monoclinic modification L3-T_O(MX-1) is formed whose satellite reflections at $h+0.663\ k\ l-0.498$ indicate an incommensurate modulation (Hoffmann et al. 1983). The modulation mainly consists of transverse wavy shifts of the tetrahedra with the wavefront parallel to the $40\bar{3}$ lattice plane (Löns and Hoffmann 1987; Graetsch and Topalovic-Dierdorf 1996).

Uniaxial pressure along the pseudohexagonal **c** axis and grinding of L1-T_O(MC) crystals also cause the transformation to L3-T_O(MX-1) at room temperature (Hoffmann et al. 1983). The latter method, however, usually yields an incomplete transformation so that a mixture of L3-T_O(MX-1) and L1-T_O(MC) is obtained.

Upon heating L3-T_O(MX-1), a new phase transition at 63 °C to a pseudo-orthorhombic modification has been detected with X-ray diffraction, DSC, ^{29}Si MAS NMR spectroscopy, and infrared spectroscopy (Hoffmann et al. 1983; Wennemer and Thompson 1984; Xiao et al. 1995; Cellai et al. 1995).

The present paper focuses on the crystallographic characterization of the new intermediate high-temperature phase of L3-T_O(MX-1) by means of X-ray precession photographs. Additional experiments were carried out using X-ray powder diffraction and differential thermal analysis.

EXPERIMENTAL METHODS

Preparation

Tridymite L3-T_O(MX-1) was prepared by heating crystals of L1-T_O(MC) to 150 °C and quenching them by dropping into ethanol, which was held at −30 °C. The crystals were subsequently allowed to slowly warm to room temperature. Examination with a polarizing microscope showed that thin platy crystals with a thickness of less than about 20 μm in the direction of the pseudohexagonal **c** axis consisted entirely of L3-T_O(MX-1), which can readily be distinguished by the much lower birefringence (Kockmeyer 1983; Vach 1983), whereas most of the thicker crystals contained L1-T_O(MC). The starting material was synthetic L1-T_O(MC) with a grain size of about 0.5 mm, which had been prepared by melting a 1:1 mixture of silica and sodium tungstate at 1400 °C. The impurity content of these crystals is below 0.1 wt% (Flörke and Langer 1972).

Part of the L3-T_O(MX-1) crystals was pulverized by grinding to obtain powder samples for X-ray powder diffraction and differential thermal analysis. Inspection of the X-ray diffractograms confirmed that the powder was pure L3-T_O(MX-1) i.e., that the sample did not contain cristobalite or another tridymite modification (cf. Fig. 2).

To obtain a powder of pure L1-T_O(MC) for comparison purposes, part of the previously investigated L3-T_O(MX-1) powder was annealed at various temperatures and slowly cooled to room temperature. A temperature of 900 °C and the presence of some Na_2WO_4 was found to be necessary for complete conversion by recrystallization. The sodium tungstate was thereafter removed from the sample by repeated washing with hot water.

Precession photographs

Buerger precession photographs taken at precession angles of 20° or 30° revealed that the L3-T_O(MX-1) crystals are pseudohexagonal twins consisting of three or more individuals. In most cases unfiltered Mo-radiation was used at an exposure time of 48 h to record the weak satellite reflections with sufficient intensity. The crystals

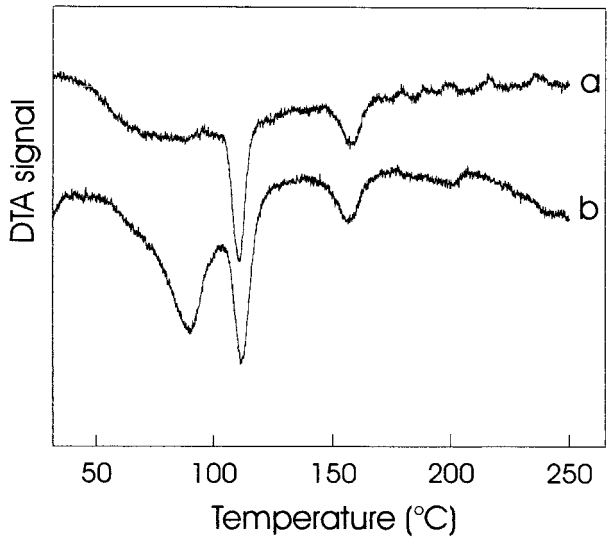

FIGURE 2. DTA curves of (**a**) L1-T_O(MC) and (**b**) L3-T_O(MX-1) recorded on heating. The onset temperatures of the DTA effects are 81, 111, and 148 °C for L3-T_O(MX-1) and 110 and 158 °C for L1-T_O(MC).

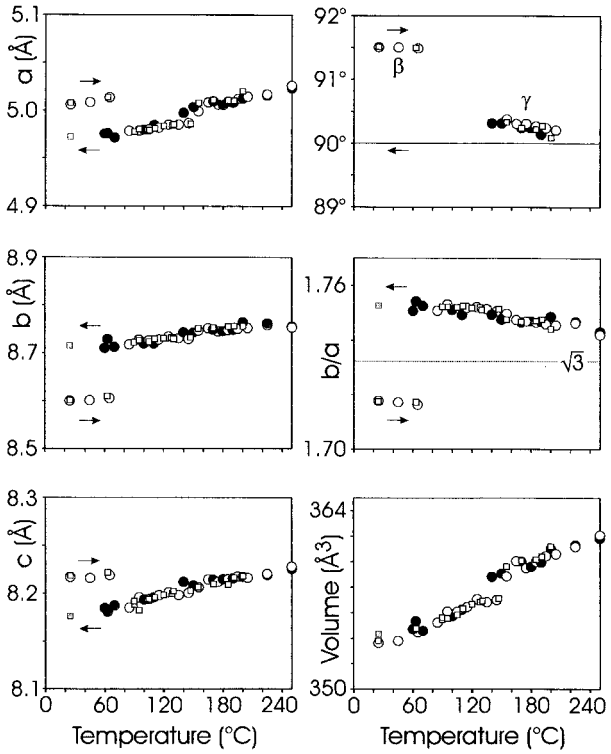

FIGURE 3. Thermal expansion of the basic structure of tridymite L3-T_O(MX-1). The lattice parameters were obtained with an X-ray powder diffractometer (squares) and a Guinier-Lenné camera (circles) on heating (open symbols) and cooling (filled symbols). The gray squares belong to traces of the orthorhombic high-temperature phase persisting at room temperature. Only data points for angles deviating from 90° are shown.

had been mounted parallel or perpendicular to the pseudohexagonal **c** axis so that *hk*0, 0*kl*, and *h*0*l* layers could be recorded. Additionally, higher level *hkl* photographs with $l = \delta_c$, $1 - \delta_c$, and 1 were taken at 90 °C (with $\delta_c = 0.388$). Cone axis images were recorded using a Zr filter at an exposure time of 24 h.

The heating experiments were conducted with a Huber resistance heater in steps of 10 °C. The crystals were placed very close to the thermocouple and a Mylar foil was wrapped around the heating device to avoid a thermal gradient or a deviation from the indicated temperature. The temperature was stable within ±1 °C during the exposure.

Powder diffraction

X-ray powder diffractograms were recorded with a Siemens D5000 diffractometer with a modified Debye-Scherrer geometry, using monochromatic Cu$K\alpha_1$ radiation and a position sensitive detector. The sample was placed in a glass capillary with a diameter of 0.3 mm. The diagrams were recorded in the stepscan modus with step sizes of 0.008° 2θ and a counting rate of 800 s per step. The glass capillary was heated with a hot air jet. Three scans were recorded at each temperature and showed no deviations from each other and no significant broadening of the reflection profiles. A static temperature gradient in the irradiated part of the capillary could not be avoided and the precision was as low as about ±15 °C in the investigated temperature range. For comparison with the lattice parameters a common setting was chosen for all phases so that $a \approx a_{hex}$, $b \approx \sqrt{3}\, a_{hex}$, and $c \approx c_{hex}$. Quartz was taken as internal standard for lattice parameter refinements. The largest estimated standard deviation is ±0.003 Å. The refined lattice parameters (Fig. 3) are consistent with those obtained at a rate of 6 °C/h using a continuously operating Guinier-Lenné camera (Graetsch and Flörke 1991).

Differential thermal analyses

DTA curves of L3-T_O(MX-1) and L1-T_O(MC) were recorded in the range of 25 to 250 °C in normal air atmosphere with a Linseis L80 thermoanalyzer at a rate of 5 °C/min. Aliquots were 200 mg samples and α-Al_2O_3 was used as the reference.

Results and interpretation

Thermal heat effects

Upon heating, the DTA curve of L3-T_O(MX-1) exhibits three major endothermic effects at onset temperatures of 81 ± 3, 111 ± 4, and 148 ± 4 °C and a much less clearly resolved minor effect near 200 °C (Fig. 4). The curve obtained on cooling showed only very sluggish effects so that hysteresis could not be measured. The broad low temperature peak is missing in the DTA curve of L1-T_O(MC). The onset temperatures of the remaining effects are 110 ± 2 and 158 ± 2 °C for L1-T_O(MC). The peak areas of the heat effects near 110 °C and 150 °C are ap-

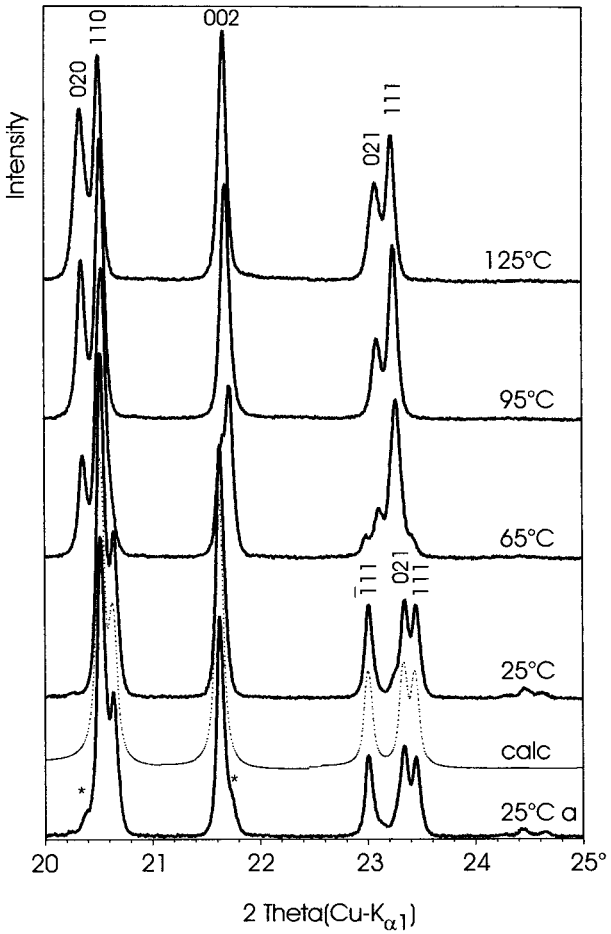

FIGURE 4. Details of X-ray powder diffractograms at various temperatures showing the change from the monoclinic room-temperature phase L3-T_O(MX-1) to the new orthorhombic high-temperature phases. The curve recorded at 65 °C exhibits reflections of both phases. The bottom curve (25 °C a) was obtained after heating to 125 °C and cooling to room temperature. The stars denote poorly resolved peaks that stem from traces of the orthorhombic high-temperature phase persisting at room temperature. The second room-temperature (25 °C) diffractogram was recorded before heating. The dotted trace was calculated without satellite reflections from the atomic coordinates of the average structure of L3-T_O(MX-1) (Graetsch and Topalovic-Dierdorf 1996).

proximately the same for both L3-T_O(MX-1) and L1-T_O(MC).

The transformation temperatures for L1-T_O(MC) are slightly lower than those of 117 and 163 °C obtained with DTA by Shahid and Glasser (1970) and 115 and 165 °C by Flörke and Müller-Vonmoos (1971). The additional broad thermal effect in the DTA curve of L3-T_O(MX-1) near 80 °C is assumed to be due to the expected transformation to the new pseudo-orthorhombic phase, but the transformation temperature is significantly higher than 63 °C as measured by Hoffmann et al. (1983) with single-crystal X-ray diffraction. Hoffmann et al. (1983) reported that the transformation temperature of L3-T_O(MX-1) considerably varies for different crystals, which probably may also explain the broadness of the DTA signal of the powder.

Thermal expansion

The X-ray powder diffractograms show that L3-T_O(MX-1) transforms at about 65 °C upon heating to a phase with an orthorhombic metric as reported by Hoffmann et al. (1983). The transformation is characterized by a sharp drop of the *c* and *a* lattice parameters (Fig. 3). Simultaneously, the *b* parameter increases so that the unit-cell volume shows no clear discontinuity at the transformation temperature. Below the phase transition, the monoclinic angle does not change before it discontinuously drops from 91.5° to 90° at the transformation temperature. Neither the position nor the intensity of the satellite reflections change significantly below the phase transition and the satellites discontinuously disappear at the inversion temperature indicating a first order transformation.

Upon cooling, the transformation does not occur at a sharp transition temperature but shows a large hysteresis of more than 10 °C and is spread over at least a further 30 °C. Traces of the orthorhombic high-temperature phase are still detectable in the X-ray powder diffractogram at room temperature (bottom curve in Fig. 2) whereas the major part of the sample returned to the original monoclinic room-temperature phase L3-T_O(MX-1). Regrinding yields pure L3-T_O(MX-1) again.

Single crystals behave differently on cooling from above the phase transition and transform to monoclinic L1-T_O(MC) or an intergrown mixture of L1-T_O(MC) and L3-T_O(MX-1) (cf. Hoffmann et al. 1983) prohibiting further investigation of the transformation behavior of L3-T_O(MX-1). As mentioned in the experimental section, transformation of L3-T_O(MX-1) powder to L1-T_O(MC) is more difficult and requires prolonged annealing at at least 900 °C and the presence of alkali ions.

Near 150 °C a small monoclinic angle of 90.36(3)° opens in the *a-b* plane, which is clearly recognizable in both powder diffractograms (Fig. 5) and Guinier-Lenné photographs (Graetsch and Flörke 1991) by the splitting of pairs of reflections into three peaks (except for 00*l* reflections). The *a* lattice parameter and the unit-cell volume show a small discontinuity (Fig. 3). With Guinier-Lenné photographs a hysteresis of about 10 °C had been found indicating a first-order character for the transformation. At higher temperatures, the monoclinic angle linearly closes approaching 90° at approximately 200 °C where the well-known orthorhombic high-temperature modification of tridymite H2-T_O(OC) is formed (cf. Dollase 1967; Kihara et al. 1986a). The exact transformation temperature is difficult to measure with X-ray diffraction because of the continuous character of the transition.

Tridymite is one of the rare examples where a high-temperature form has a lower symmetry than the preced-

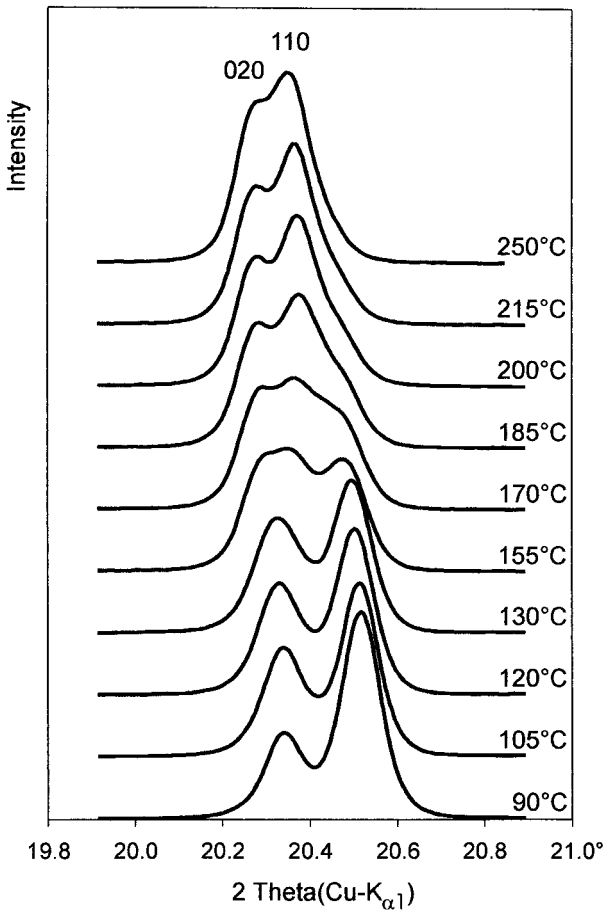

FIGURE 5. Details of X-ray powder diffractograms at elevated temperatures showing the splitting of the 020 and 110 reflections of the orthorhombic high-temperature phases into three components due to the formation of an intermediate monoclinic phase between 150 and 200 °C.

ing low-temperature modification and L3-T_o(MX-1) shows the following sequence of transformations:

$$\text{monoclinic} \xrightarrow{65\ ^\circ\text{C}} \text{orthorhombic} \xrightarrow{150\ ^\circ\text{C}} \text{monoclinic} \xrightarrow{200\ ^\circ\text{C}} \text{orthorhombic}$$

For the chosen setting, the monoclinic angle is β at room temperature and γ for the intermediate high-temperature form. The DTA peaks at 81 and 148 °C can be assigned to first-order transformations observed as discontinuities of the lattice parameters at about 65 and 150 °C. The difference in the temperature of the first transformation as measured with X-ray diffraction and DTA can probably be explained by overheating due to the faster heating rate of 5 °C per minute for the DTA experiment as compared with 5 °C per hour for the Guinier-Lenné photographs and the stepwise heating for powder diffractometry. The transition that gives rise to the thermal effect at 111 °C, however, is not detected in the thermal expansion behavior.

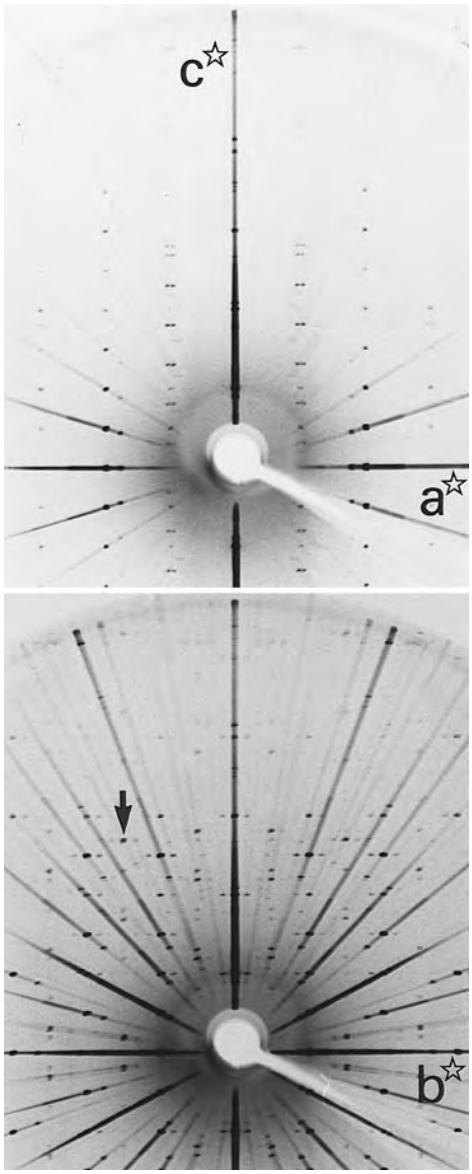

FIGURE 6. Precession photographs recorded at 95 °C with white Mo-radiation at a precession angle of 30°. At the bottom: 0*kl* plane with *b* and *a-c* satellites. The arrow point to an *a-c* satellite reflection (with $k = 3$) that is surrounded by *b* satellites. At the top: *h*0*l* plane with split *a-c* satellites and additional weak P reflections on reciprocal lattice rods parallel to **c*** with an odd *h* index.

Displacive modulations

Precession photographs taken between 65 and 115 °C reveal several systems of extra reflections (Figs. 6, 7, and 8). The main reflections of the orthorhombic sublattice are surrounded by single pairs of satellite reflections parallel to **b*** (in the following referred to as *b* satellites). The distance of the satellites from the main reflections is ⅓ *b** indicating a commensurate modulation (superstructure) with tripled *b* lattice parameter. Main reflections

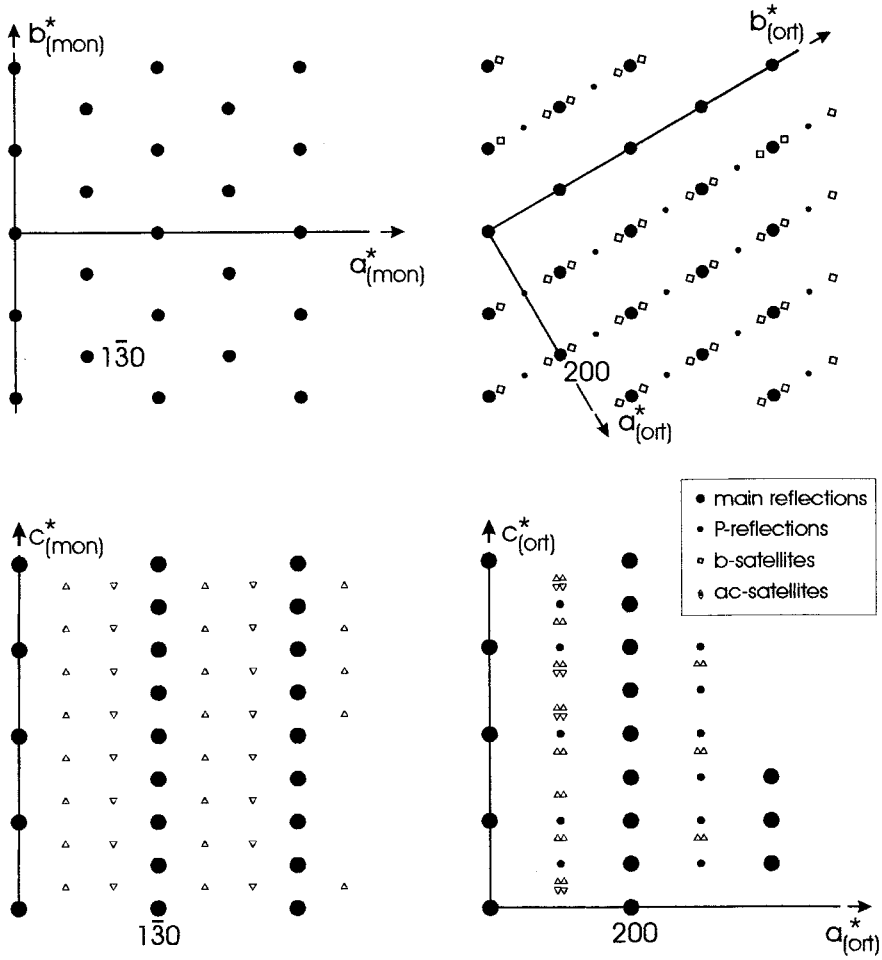

FIGURE 7. Schematic representation of corresponding diffraction patterns of monoclinic L3-T_O(MX-1) (on the left side) and the new incommensurate orthorhombic tridymite modification existing between 65 and 110 °C (on the right side).

with 0*k*0 do not have *b* satellites (Fig. 7). Visual inspection of the *hk*0 plane (Fig. 8) shows that the intensity of the satellite reflections increases with the *h* indices at the expense of the main reflections. The direction of the modulation (along **b***) is perpendicular to the direction of the intensity variation (parallel to **a***) indicating that the modulation consists of transverse wavy displacements of the atoms (Korekawa 1967).

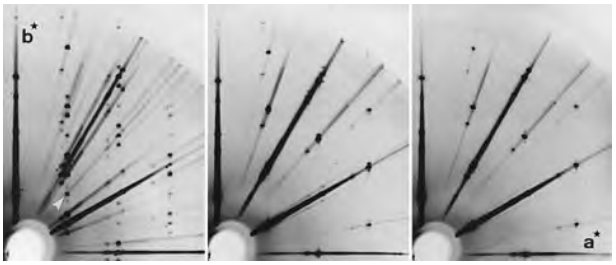

FIGURE 8. Details of precession photographs recorded at 105, 135, and 185 °C (from the left to the right side) showing *b* satellites surrounding the main reflections at $\delta_b = ⅓$ in the *hk*0 plane. The arrow points to an additional P reflection (120) associated with a pair of *b*′ satellites at $\delta_{b'} = ¼$.

In the 0*kl* plane (Fig. 6), additional extra spots occur on reciprocal lattice rods parallel to **c*** with odd *k* index. The positions of these reflections are $l \pm 0.388$ indicating an incommensurate modulation along **c***. In the *h*0*l* plane (Fig. 6), the extra spots occur on lattice rods with odd *h* index. Splitting of the satellites along **a*** is visible showing that the wavevector of the modulation has an additional small non-integer component of $\delta_a = \pm 0.042$. This shows that the satellites do not exactly lie on the 0*kl* plane but are close enough to pass through the zero level screen and appear as extra spots on the 0*kl* photograph. The intensities of the satellites seem to increase with the *l* index indicating a contribution of longitudinal displacements to the modulation (Korekawa 1967). The extra reflections (referred to as *a*-*c* satellites) also have been found in cone axis photographs, in *hk*δ_c and *hk*1-δ_c planes and in powder diffractograms with long exposure time. The *a*-*c* satellites are surrounded by weak *b* satellites

(Fig. 6). Their positions do not depend on the temperature within the obtained accuracy of $\Delta\delta \approx \pm 0.003$. The diffraction patterns are schematically illustrated in Figure 7 together with the corresponding patterns of the room-temperature phase L3-T_O(MX-1).

In the *h*0*l*, *hk*0, and *hk*1 planes additional weak reflections were found with $h + k = 2\,n + 1$, which reveals that the *C* centering of the sublattice is destroyed (referred to as P reflections). These reflections are surrounded by pairs of satellites parallel to **b*** at a position of $\delta_{b'} = \pm$ ¼ (Fig. 8). Due to their very low intensity only very few of these *b*′ satellites could be found in the *hk*0 and *hk*1 planes and the dependence of their intensity on the diffraction angle could not be examined. Their position seems to be independent from the temperature like the *b* and the *a*-*c* satellites.

The diffraction pattern of the main reflections is consistent with space group $P2_12_12_1$. Thus, symmetry and superstructure with tripled **b**-axis strongly resemble those of H4-T_O(OP) that is known as an intermediate high-temperature phase of L1-To(MC) occurring in the temperature range from about 115 °C to 160 °C (Table 1; Kihara 1977; Nukui et al. 1978). The arrangement of *a*-*c* satellites, on the other hand, is somewhat similar to the diffraction pattern of L2-T_D($PO_{5/10}$) as reported by Hoffmann et al. (1983) but clearly differs by the incommensurate location of the *a*-*c* satellites with respect to the underlying sublattice. Because the *b* satellites also surround *a*-*c* satellites both (commensurate and incommensurate) modulations are not independent from each other, e.g., do not belong to different domains but rather form a two-dimensional modulation with commensurate and incommensurate components. Compared with the room-temperature phase, the initial modulation changed the direction and is apparently split into a component parallel to **b*** and a second approximately parallel to **c*** (Fig. 7). The phase found in the temperature ranges from 65 to 110 °C, thus, in spite of the similarities with other forms of tridymite, it represents a new modification of tridymite.

Above 110 °C, the *a*-*c* satellites and the P reflections as well as their *b*′ satellites are absent indicating that the incommensurate part of the modulation disappeared and that the *C* centering is restored (Fig. 8). Simultaneously, the *b* satellites moved from $\delta_b = ⅓$ to 0.077 disclosing that the commensurate part of the modulation along **b*** survived but became incommensurate with a wavelength of 115 Å. Several new higher orders of satellite reflections are visible. The wavelength of the modulation gradually decreases with increasing temperature to about 100 Å at 155 °C (Fig. 9). The symmetry of the diffraction pattern is consistent with the space group $C222_1$ for the basic structure.

Although the shape and volume of the unit cell do not change during the transition, the heat effect at 110 °C and the discontinuous disappearance of the *a*-*c* satellites and the P reflections indicate that the transformation is first order. The symmetry of the basic structure is the same as that of the orthorhombic high-temperature phase [H2-T_O(OC)] existing above 200 °C (Dollase 1967). Whereas the new phase exhibits sharp satellite reflections, H2-T_O(OC) shows a complicated pattern of streaks with diffuse intensity in electron diffraction patterns (cf. Withers et al. 1994). The orthorhombic phase between 110 and 155 °C represents a new incommensurate modification of tridymite with very close similarity to incommensurate H3-T_O(OS). It might be a discommensurate phase with a discontinuous modulation consisting of almost commensurate domains separated by discommensurate domain walls. Further experiments are necessary to reveal the microscopic nature of this modification.

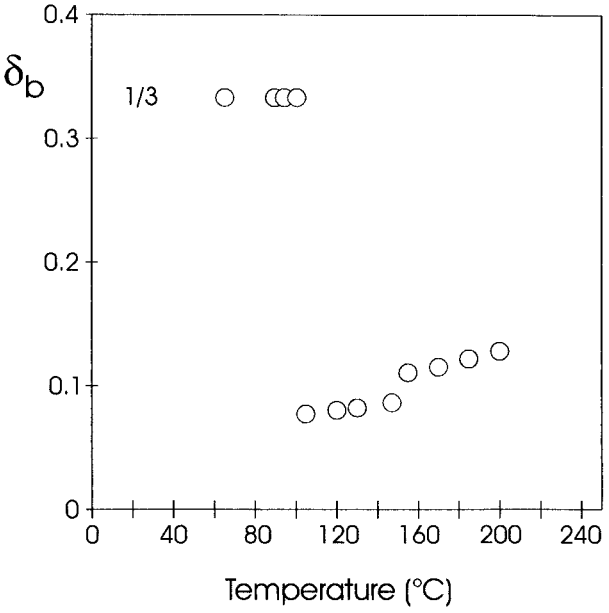

Figure 9. Component of the modulation vector $\mathbf{q}_b = \delta_b$ **b*** at various temperatures. The modulation is commensurate with $\delta_b = ⅓$ and independent of the temperature between 65 and 110 °C and incommensurate between 110 and 200 °C with changing linear dependence of δ_b on the temperature near 150 °C.

The small monoclinic angle of H3-T_O(OS) in the temperature range from 155 to about 200 °C is hardly visible in the precession photographs. Nevertheless, the space group symmetry of the basic structure is reduced from $C222_1$ to $C112_1$. (The latter can be transformed to the conventional setting in space group $P112_1$, no. 4 with a smaller unit cell by appropriate change of the axes.) Only single pairs of first-order satellites remain visible (Fig. 8). The modulation wavevector linearly increases with increasing temperature as in the preceding incommensurate phase but with a steeper slope (Fig. 9). The intensity of the satellites gradually decreases with increasing temperature and fades into very weak diffuse streaks connecting the main reflection near 200 °C.

The H3-T_O(OS) phase of L3-T_O(MX-1) is identical with the corresponding intermediate high-temperature phase of L1-T_O(MC) occurring in approximately the same temperature interval. The experimental results are sum-

TABLE 2. Tranformation sequence of tridymite L3-T_O (MX-1) upon heating

Transition temperature (°C)	Phase	Space group of the basic structure	Wave vector of the modulation
	H1-T_O (HP)*	$P6_3/mmc$	—
≈380			
	H2-T_O (OC)†	$C222_1$	—
≈200			
	H3-T_O (OS)‡	$C112_1$	$\delta_b b^*$; δ_b = 0.10 to 0.14
150			
	H5-T_O§	$C222_1$	$\delta_b b^*$; δ_b = 0.08 to 0.09
110			
	H6-T_O§	$P2_12_12_1$	0.042 a* − 0.388 c* 1/3 b*; (1/4 b*)
65			
	L3-T_O (MX-1)‖	Cc	0.663 a* − 0.498 c*

Note: H = high temperature, L = low temperature, $_O$ = ordered; in parentheses: H = hexagonal, O = orthorhombic, M = monoclinic, C = C-centered unit cell, S = (incommensurate) superstructure.
* Gibbs (1927); Kihara (1978).
† Dollase (1967); Kihara et al. (1986a).
‡ Nukui et al. (1979); Graetsch and Flörke (1991).
§ This work.
‖ Hoffmann et al. (1983); Löns and Hoffmann (1987).

marized in Table 2. As far as can be seen from the X-ray powder diffraction patterns, the high-temperature phases H2-T_O(OC) and H1-T_O(HP) of L3-T_O(MX-1) are also identical with the corresponding high-temperature phases of L1-T_O(MC) Graetsch and Flörke (1991). The new intermediate incommensurate phases are labeled in Table 2 as H6-T_O and H5-T_O.

DISCUSSION

Tridymite is formed at high temperatures either hydrothermally or from an alkali-containing melt. At 465 °C an onset of spontaneous strain parallel to **c** has been detected by De Dombal and Carpenter (1993). The hexagonal-orthorhombic transformation near 350 °C is associated with additional spontaneous strain perpendicular to **c**. Below 250 °C, tridymite shows behavior typical of incommensurate dielectrics (Janssen 1986): continuous transformation of the parent structure [in the case of tridymite: H2-T_O(OC)] to an incommensurate phase [H3-T_O(OS)] followed by a lock-in transition to a commensurate superstructure [H4-T_O(OP)]. The latter transformation is discontinuous for tridymite. In most cases, the formation of an incommensurate phase is driven by a soft mode and consequently Nukui et al. (1979) postulated the condensation of a soft mode for H3-T_O(OS) resulting in a transverse wavy displacement of the tetrahedra from the positions of the parent or basic structure. However no attempt has been undertaken to investigate the lattice dynamics of tridymite to date with respect to soft modes. The lock-in transition seems to be lacking in some crystals (Dollase 1967; Cellai et al. 1994) that might depend on the thermal history of the particular crystals or be due to the presence of impurities and other structural defects.

The transformation behavior of tridymite below 120 °C is even more interesting and results in at least three different modifications existing at room temperature. Traces of a further incommensurate room-temperature modification have apparently been produced by Withers et al. (1994) by a high-temperature electron diffraction investigation. Upon slow cooling single crystals of ordered tridymite, the superstructure of L1-T_O(MC) is formed. [The presence of stacking faults directs the transition to pseudo-orthorhombic tridymite L2-T_D($PO_{5/10}$).] Stress, either introduced thermally by quenching or mechanically by grinding obviously causes some kind of a ''lock-out'' transition resulting in incommensurate L3-T_O(MX-1). The X-ray densities of the tridymite polymorphs increase in the order: L2-T_D($PO_{5/10}$) > L1-T_O(MC) > L3-T_O(MX-1) > H4-T_O(OP) etc. placing the quenched phase intermediate between the other room-temperature modifications and the high-temperature forms of tridymite.

Upon heating L3-T_O(MX-1), the first transformation occurs by 65 °C. Obviously, the strain release is insufficient to restore the lock-in phase H4-T_O(OP). A series of two similar orthorhombic phases is formed instead: one with an temperature independent additional incommensurate component to the modulation (H6-T_O) and a second with another temperature dependent incommensurate modulation (H5-T_O). The latter is replacing H4-T_O(OP) in its original temperature range. At higher temperatures the old transformation sequence consisting of incommensurate H3-T_O(OS), normal H2-T_O(OC), and H1-T_O(HP) is followed. But renewed cooling reveals some memory effect and L3-T_O(MX-1) is at least partly formed again instead of L1-T_O(MC). The memory effect is much stronger in powder particles than in larger crystals indicating that the particle or domain size has an important influence on the direction of the back-transformation, presumably through pinning at surfaces or other defects.

In microscopic theory, competing short-range interactions are generally considered as responsible for the formation of incommensurate states in dielectrics (cf. Sannikow 1986; Janssen 1986). The most striking configurational difference in the local arrangements of the tetrahedra in tridymite and cristobalite had been pointed out by Gibbs (1927) and Flörke (1967). Potentially conflicting forces can readily be detected so that a conceptual picture can be drawn. In idealized high cristobalite (with Si-O-Si angles of 180°), all tetrahedra are in mutual trans-configuration. In idealized high tridymite, each tetrahedron has three neighboring tetrahedra in trans-configuration and one in a cis-configuration. The intertetrahedral O-O distances are maximal in the trans-configuration and minimal in the cis-configuration causing minimal and maximal repulsion among the tetrahedra, respectively (Flörke 1967).

In tridymite, the different local repulsive forces in both kinds of configurations are apparently conflicting in following the common tendency of the interconnected rigid tetrahedra for maintaining unstrained intertetrahedral Si-O-Si angles of around 145°. As a consequence, the Si-O-Si angles are larger in cis- than in trans-configuration of the various tridymite modifications (Flörke 1967; Kihara

1977) indicating different success in this competition. At high temperatures, straight Si-O-Si angles are avoided through thermal vibrations of the tetrahedra (Kihara et al. 1986b; Dove et al. 1996). At lower temperatures, sufficiently small Si-O-Si angles are yielded by the formation of superstructures or displacive modulations. In cristobalite, the local environment is the same for all tetrahedra and upon cooling from high temperatures a stable arrangement is achieved in a single step by cooperative distortions of the rings of tetrahedra (Peacor 1973; Schmahl et al. 1992). The different tetrahedral configurations in tridymite, however, cause more complicated patterns of cooperative distortions that are less stable and appear to be sensitive to defects, external stress, and structural strain. The successful formation of the lock-in phase [H4-T_o(OP)] and the passage through the temperature range of 150 and 110 °C seem to be most critical for the direction of the transformation path at lower temperatures.

Acknowledgments

I thank O.W. Flörke for the L1-T_o(MC) tridymite crystals, B. Marler and S. Vortmann for recording the powder diffractograms, and O.W. Flörke, C. Fyfe, H. Gies, and K. Kihara for reviewing the manuscript.

References cited

Baur, W.H. (1977) Silicon-oxygen bond lengths, bridging angles Si-O-Si and synthetic low tridymite. Acta Crystallographica, B33, 2615–2619.

Cellai, D., Carpenter, M.A., Wruck, B., and Salje, E.K.H. (1994) Characterization of high-temperature phase transitions in single crystals of Steinbach tridymite. American Mineralogist, 79, 606–614.

Cellai, D., Carpenter, M.A., Kirkpatrick, R.J., Salje, E.K.H., and Zhang, M. (1995) Thermally induced phase transitions in tridymite: an infrared spectroscopy study. Physics and Chemistry of Minerals 22, 50–60.

De Dombal, R.F. and Carpenter, M.A. (1993) High-temperature phase transitions in Steinbach tridymite. European Journal of Mineralogy, 5, 607–622.

Dollase, W.A. (1967) The crystal structure at 220 °C of orthorhombic high tridymite from the Steinbach meteorite. Acta Crystallographica, 23, 617–623.

Dollase, W.A. and Baur, W.H. (1976) The superstructure of meteoritic low tridymite solved by computer simulation. American Mineralogist, 61, 971–978.

Dove, M.T., Hammonds, K.D., Heine, V., Withers, R.L., Xiao, Y., and Kirkpatrick, R.J. (1996) Rigid unit modes in the high-temperature phase of SiO_2 tridymite: calculations and electron diffraction. Physics and Chemistry of Minerals, 23, 56–62.

Flörke, O.W. (1967) Die Modifikationen des SiO_2. Fortschritte der Mineralogie, 44, 181–230.

Flörke, O.W. and Langer, K. (1972) Hydrothermal recrystallization and transformation of tridymite. Contributions to Mineralogy and Petrology, 26, 221–230.

Flörke, O.W. and Müller-Vonmoos, M. (1971) Displazive Tief-Hoch-Umwandlung von Tridymit. Zeitschrift für Kristallographie, 133, 193–202.

Flörke, O.W. and Nukui, A. (1988) Strukturelle Pathologie von Tridymiten. Neues Jahrbuch für Mineralogie Abhandlungen, 158, 175–182.

Graetsch, H. and Flörke, O.W. (1991) X-ray powder diffraction and phase relationship of tridymite modifications. Zeitschrift für Kristallographie, 195, 31–48.

Graetsch, H. and Topalovic-Dierdorf, I. (1996) 29Si MAS NMR spectrum and superstructure of modulated tridymite L3-T_o(MX-1). European Journal of Mineralogy, 8, 103–113.

Gibbs, R.E. (1927) The polymorphism of silicon dioxide and the structure of tridymite. Proceedings of the Royal Society of London, A113, 351–368.

Hoffmann, W. (1967) Gitterkonstanten und Raumgruppe von Tridymit bei 20 °C. Naturwissenschaften, 54, 114.

Hoffmann, W., Kockmeyer, M., Löns, J., and Vach, C. (1983) The transformation of monoclinic low-tridymite MC to a phase with an incommensurate superstructure. Fortschritte der Mineralogie, 61, 96–98.

Janssen, T. (1986) Microscopic theories of incommensurate crystal phases. In R. Blinc and A.P. Levanyuk, Eds., Incommensurate Phases in Dielectrics 1. Fundamentals, p. 67–142. North-Holland Publications, Amsterdam.

Kato, K. and Nukui, A. (1976) Die Kristallstruktur des monoklinen Tief-Tridymits. Acta Crystallographica, B32, 2486–2491.

Kihara, K. (1977) An orthorhombic superstructure of tridymite existing between about 105 and 180 °C. Zeitschrift für Kristallographie, 146, 185–203.

———(1978) Thermal change in unit cell dimensions and a hexagonal structure of tridymite. Zeitschrift für Kristallographie, 148, 237–253.

Kihara, K., Matsumoto, T., and Imamura, M. (1986a) Structural change of orthorhombic-I tridymite with temperature: a study based on second order thermal-vibrational parameters. Zeitschrift für Kristallographie, 177, 27–38.

———(1986b) High-order thermal motion tensor analyses of tridmite. Zeitschrift für Kristallographie, 177, 39–52.

Kockmeyer, M. (1983) Präparation, Kristalloptik und gesetzmäβige Verwachsungen der Tridymitmodifikationen MC, MX-1 und M. Diplomarbeit, Westfälische Wilhelms-Universität Münster.

Konnert, J.H. and Appleman, D.E. (1978) The crystal structure of low tridymite. Acta Crystallographica, B34, 391–401.

Korekawa, M. (1967) Theorie der Satellitenreflexe. Habilitationsschrift, Ludwig Maximilians Universität München.

Löns, J. and Hoffmann, W. (1987) Zur Kristallstruktur der inkommensurablen Raumtemperaturphase des Tridymits. Zeitschrift für Kristallographie, 178, 141–143.

Nukui, A., Nakazawa, H., and Akao, M. (1978) Thermal changes in monoclinic tridymite. American Mineralogist, 63, 1252–1259.

Nukui, A., Yamamoto, A., and Nakazawa, H. (1979) Non-integral phase in tridymite. In J.M. Cowley, J.B. Cohen, M.B. Salamon, and B.J. Wuensch, Eds., Modulated Structures. American Institute of Physics Conference Proceedings, 53, 327–329.

Peacor, D.R. (1973) High-temperature single-crystal study of the cristobalite inversion. Zeitschrift für Kristallographie, 138, 274–298.

Sannikow, D.G. (1986) Phenomenological theory of the incommensurate-commensurate phase transition. In R. Blinc and A.P. Levanyuk, Eds., Incommensurate Phases in Dielectrics 1. Fundamentals, p. 43–65. North-Holland Publication, Amsterdam.

Schmahl, W.W., Swainson, I.P., Dove, M.T., and Graeme-Barber, A. (1992) Landau free energy and order parameter behaviour of the α/β phase transition in cristobalite. Zeitschrift für Kristallographie, 201, 125–145.

Shahid, K.A. and Glasser, F.P. (1970) Thermal properties of tridymite: 25–300 °C. Journal of Thermal Analyses, 2, 181–190.

Tagai, T., Sadanaga, R., Takeuchi, Y., and Takea, H. (1977) Twinning of tridymite from the Steinbach meteorite. Mineralogical Journal of Japan, 8, 382–398.

Vach, C. (1983) Tridymit MX-1, eine Tridymitmodifikation mit inkommensurabler Überstruktur. Diplomarbeit, Westfälische Wilhelms-Universität Münster.

Wennemer, M. and Thompson, A.B. (1984) Ambient temperature phase transitions in synthetic tridymites. Schweizerische mineralogische und petrographische Mitteilungen, 64, 355–368.

Withers, R.L., Thompson, J.G., Xiao, Y., and Kirkpatrick, R.J. (1994) An electron diffraction study of the polymorphs of SiO_2-tridymite. Physics and Chemistry of Minerals, 21, 421–433.

Xiao, Y., Kirkpatrick, R.J., and Kim, Y.J. (1995) Investigations of MX-1 tridymite by ^{29}Si MAS NMR-modulated structures and structural phase transitions. Physics and Chemistry of Minerals, 22, 30–40.

Manuscript received June 3, 1997
Manuscript accepted January 25, 1998
Paper handled by Simon A.T. Redfern